

# Performance testing of selected automated coastline detection techniques applied on multispectral satellite imageries

Shreyashi Santra Mitra<sup>1</sup> · D. Mitra<sup>2</sup> · Abhisek Santra<sup>1</sup>

Received: 10 February 2016 / Accepted: 23 January 2017 / Published online: 13 February 2017  
© Springer-Verlag Berlin Heidelberg 2017

**Abstract** Coastline detection has been of major interest for environmentalists and many methods have been introduced to detect coastline automatically. Remote Sensing techniques are the most promising ones to deliver a satisfactory result in this regard. In our study, the objective was to retrieve performance level of certain image processing techniques vigorously used for the purpose to delineate coastline automatically and they were tested against two images acquired almost on the same period by LISS III and LANDSAT ETM+ sensors. The algorithms used in the study are Water Index, NDVI, Complex Band Ratio, ISODATA, Thresholding, ISH Transformation techniques. Accuracy of the shoreline detection by classifying the image in land and water has been tried to be estimated in three ways, firstly with comparison to the visually interpreted high resolution google earth image, secondly field collected GCP data of reference points of classes and thirdly the raw image itself. But problem in temporal disparity caused the constraint doing accuracy assessment from the first two reference data and maps along the coast. As a whole although four techniques among six, show satisfactory results namely density slicing, ISODATA classification, Water Index and ISH transformation technique, in the case of LISS-III and ETM+, Water Index (with kappa value being 0.95 for LISS-III and 0.97 for ETM+) and Intensity-Hue-Saturation transformation techniques give better performance. Sensor to sensor variation

might have introduced certain differences in shoreline detection in images of same season with similar tidal influence.

**Keywords** Coastline · Remote sensing · Image processing · Water index · Kappa statistics · Accuracy

## Introduction

Coastal erosion monitoring is one of the important research areas of the environmentalists for the sake of the protection of the coastal environment and the population residing on this transitional terrain. Coastline mapping and change detection are on the other hand essential for safe navigation, resource management, environmental protection, sustainable coastal development and planning (Di et al. 2003; Ahmad and Lakhan 2012). Application of conventional ground survey (like coastline demarcation using instrumental survey like DGPS with ARC PAD) to measure the position of shoreline is both labour intensive and time consuming. To substitute this process, Remote Sensing data can be used. Both finer and coarser resolution photographs and images are useful for the study of coastal accretion and erosion because they provide us with instantaneous snapshots of the study area (Santra et al. 2011). However, choosing the right kind of satellite imagery and as well as the technique to detect coastline for monitoring shoreline changes have now become some of the biggest challenges to the scientists (Aedla et al. 2015). These challenges owe to the fact that different satellites with varying temporal repeativity have different sensor characteristics in terms of their spatial, spectral and radiometric resolution. The time of image acquisition is important to identify coastline as coastline detection becomes complex task considering the tidal effect on the coasts which makes the shoreline most unpredictable and accurately unidentifiable. From remote sensing

Responsible editor: H. A. Babaie

✉ Shreyashi Santra Mitra  
shreyashi.mitra@gmail.com

<sup>1</sup> Department of Civil Engineering, Haldia Institute of Technology, East Medinipur, Haldia, India

<sup>2</sup> Indian Institute of Remote Sensing, 4, Kalidas Road, Dehradun, Uttarakhand 248001, India

techniques this problem becomes more prominent. Some portions of land may be misinterpreted as water in the images taken at high tidal phase. On the contrary the waterline could be observed substantially receded if image is taken at low tidal phase.

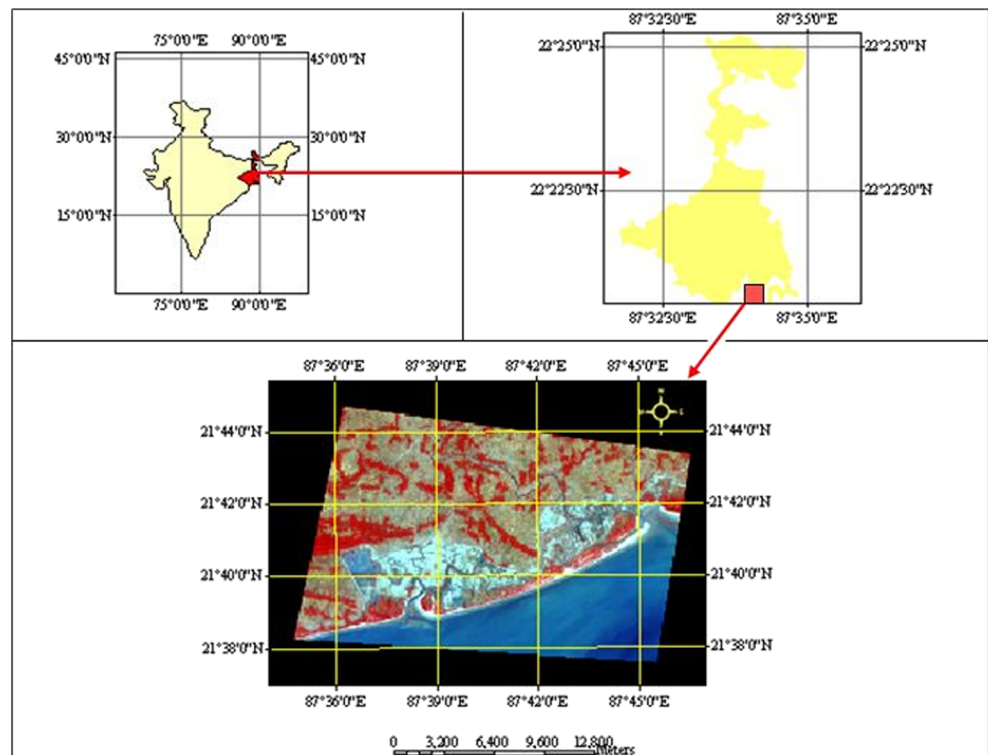
The Image-based techniques applied for the purpose of coastline detection are also various and showed different level of accuracies in different studies. Winarso and Budhiman (2001), cited the potential application of remote sensing data for coastal study. They have studied the coastal information using LANDSAT ETM+ imageries supported by LANDSAT 5 TM imageries, bathymetric maps and tidal data using easy combination of band ratio of 4/2 and 5/2 band combinations. Chang et al. (1999) used robust system for shoreline detection and studied its application to coastline detection using SPOT multispectral images. In this work they have converted the colour model of image representation from RGB to ISH and then have used the ISODATA classification to categorise additional information to obtain the coastline detection. Li et al., in (2001) attempted a comparative study on shoreline mapping techniques. In Lake Erie region using NOAA/ NGS aerial images, simulated outputs and actual IKONOS images Foody (2002) studied the role of soft classification techniques in the refinement of coastline detection methods. He proposed that a soft classification of landcover may be used to direct estimation of GCP location to track coastline and its changes. Krishna et al. (2005) worked on the evaluation of some selected semi-automated image processing techniques for identification and delineation of coastal edge using IRS-LISS-III image

Sagar Island on the East coast of India. In this work some classification techniques like level slicing, Principle Component analysis, NDVI, Water Index and ISODATA were applied and compared by accuracy assessment. Alesheikh et al. (2007) have studied coastline change detection using remote sensing techniques. Their work was based on a combination of histogram thresholding and band ratio techniques and they have estimated the extracted coastline accuracy as 1.3 pixels (pixel size equals to 30 m). There were also some works done so far to delineate the coastline using both Remote Sensing and GIS methods (Ahmad and Lakhan (2012), (Tran Thi et al. (2014) with some reliable outputs. It is evident that a number of works have been done so far to detect coastline and understand its dynamism in relation to it. However, comparative assessment of the performance of some most exhaustive and reliable semi automated techniques applied on two different sensor based products is not frequent, though important. In this work, the authors have tried to analyse performance of these methods on two images of different sensors for better understanding the efficiency of each of the techniques.

### Study Area

The coastal tract under study is mainly comprised of the Mandarmani coast which is also known as Dadanpatrabar Coast and Shankarpur coast. Mandarmani or Mandarbani is situated in the Ramnagar II Block of the Contai Sub-Division of the District of East-Medinipur in West Bengal whereas Shankarpur is situated at Digha block (Fig. 1). The west to

**Fig. 1** Geographical location of study area



east extended Shankarpur-Mandarmani tropical sandy beaches of northeastern Indian coast of Bay of Bengal covers a linear stretch of about 23 km. This area is a part of Eastern coastal tract of India and considered to be highly dynamic in terms of spatio-temporal variation with response to various coastal processes (Jana and Bhattacharya 2013). However this tract has much straighter shoreline compared to other sections of Indian coast. As this study aims to represent a comparative account of image based semi-automated shoreline detection techniques, simple linear coastal tract would give a better platform for testing than that of complex geometrically sculptured coastal stretch. Considering the fact, this part of Eastern Indian coastal stretch has been used for the study.

The elevation of the coast in the southernmost region is <3 m above the sea level (Umitsu 1993). The physiographic division falls under the low-lying flat area with feeble variation in relief. The slope ratio along the shoreline can be expressed as 1:0.005 (Hz:Vt) and across the shoreline 1:0.02 (Hz:Vt). The geological history of the coast is comparatively short and the coast is still in its formative state. Its present day situation is the consequence of fluvio-tidal and coastal processes that has resulted from the overlapping sequence of Flandrian transgression, > 5900 yrs. B.P. and overlapping sequence of delta progradation till the sea level gets stabilised at around 3000 yrs. B.P.(Chakrabarti 1990). This coastal tract has varied geomorphologic features. The beach has a linear almost east-west extension of variable width. Morphodynamically, the beach has a dissipative profile (Short 1983) with high compaction of sediments and a gently sloping gradient towards the sea. The backshore beach is featured by a number of dune trains with undulating surface. The southernmost dune tail lies along the lower marine terrace. Dunes present on the coasts are covered with halophytic creepers and herbs. When the sea recedes, the dunes move forward and change their place. The foreshore beach is generally flat, slightly concave upward to gently undulating, often with upper and lower beach faces. Surface sedimentary structures include backwash ripples, rhomboid marks, crescentic, wave- and interference ripples of ladder-back types, current crescents, rill marks and swash marks (Komar 1976). Cut-out trenches reveal alternation of seaward dipping cross-beds and parallel beds reflecting deposition from low tide and high tide respectively (Bhattacharya et al. 2003). The transition zone, in between and foreshore and backshore, changes its position in time and space depending on the fluctuation of high water spring and neap tides. This zone is characterised by a spectrum of surficial and internal, sedimentary and biogenic structures (Bhattacharya and Sarkar 2001) The soil of the study area varies from coastal fringe to the landward unit. The beach is generally composed of siliciclastic, quartzo-feldspathic material in composition with well sorted, medium to fine sand (Frey 1975). The estuarine mud near Pichhabani inlet, mixing with the beach sand creates mixed flats. The Mandarmani

beach, about 14 km long is dominated by tiny sand particles. The soil condition of the area proves that modern estuary-influenced beaches have a range of soil textural gradients and morphologies controlled by fluvial, tidal and wave regime. Tidal Influence and Tidal height experienced in the study area remains between 3 to 5 m (approximately) (Wright and Coleman 1973; Kuehl et al. 1997). Usually in the study area, situated at the East Coast of India, the horizontal shift due to the tidal difference between high tide and low tide of the sea remain 3 to 5 m (approximately) compared to 9 to 11 m at Western coast of India. Therefore this region is evidently a mesotidal zone and can be considered as mixed-energy coasts (Hayes 2005). In wave dominated and tide dominated coasts, influence of wave and tides acts as a driving force in coastal geomorphologic including its geometrical set up (Anthony 2005), whereas in mixed energy coast no tremendous dominance of wave or tide can be seen, rather the coasts are a product of both the processes. However, sometimes in mixed energy coast, slight dominance of wave or tide may be observed.

## Materials and methods

### Datasets

In this project extensive data sets were used to carry out the project. To follow the objective of finding out the best remote sensing techniques for coastline extraction, both optical and microwave images were gathered. The brief discussion about the materials used are given below.

Two satellite images were taken to accomplish the study, i.e. Landsat-7 ETM+ and IRS LISS 3 images which were acquired in the same season in 2009. The details of the image and the bands used for the study have been indicated using Tables 1 and 2.

### Methods

The entire process of shoreline detection has been structured following interrelated flow of methods. The overall methodology of the study has been shown here with the help of a flow chart (Fig. 2).

The methodology has been divided in Pre-Processing, Processing, Accuracy Assessment, Field Check.

**Table 1** Optical raw satellite image details

| Satellite | Sensor & band | Resolution (m) | Date       | Path | Row |
|-----------|---------------|----------------|------------|------|-----|
| IRS-1C    | LISS-III      | 23.5           | 06.12.2009 | 108  | 57  |
| LANDSAT   | ETM+          | 28.5           | 17.11.2009 | 138  | 045 |

**Table 2** Spectral bands used from the selected satellite images

| Landsat ETM+  |                     | IRS LISS-3    |                     |
|---------------|---------------------|---------------|---------------------|
| Spectral band | Band width (Micron) | Spectral band | Band width (Micron) |
| Pan           | 0.522–0.90          |               |                     |
| 1             | 0.45–0.53           |               |                     |
| 2*            | 0.53–0.60           | 2*            | 0.52–0.59           |
| 3*            | 0.63–0.69           | 3*            | 0.62–0.68           |
| 4*            | 0.76–0.90           | 4*            | 0.77–0.86           |
| 5*            | 1.55–1.75           | 5*            | 1.55–1.70           |
| 6             | 10.4–12.5           |               |                     |
| 7             | 2.09–2.35           |               |                     |

Footnote: Bands numbers with \* denote bands used in the study

**Image pre-processing**

In this phase all the datasets were collected from different sources and organised in a proper fashion. The Survey of India Topographical sheets of 1950 and 1963 were geo-referenced properly on ERDAS 9.1 platform in UTM projection (spheroid and datum being WGS 84, Zone 45) with nearest neighbour resampling technique using polynomial equation in 1st order. Then the portions showing the study area were subset.

In the second step all the satellite images were subset and radiometric corrections were done to avoid the errors that a

satellite image always comes with due to atmospheric or geometric distortions using Dark object Subtraction (DoS) method. Followed by this all the images were geo-referenced with respect to toposheet keeping RMS error less than 0.50 or half of pixel size.

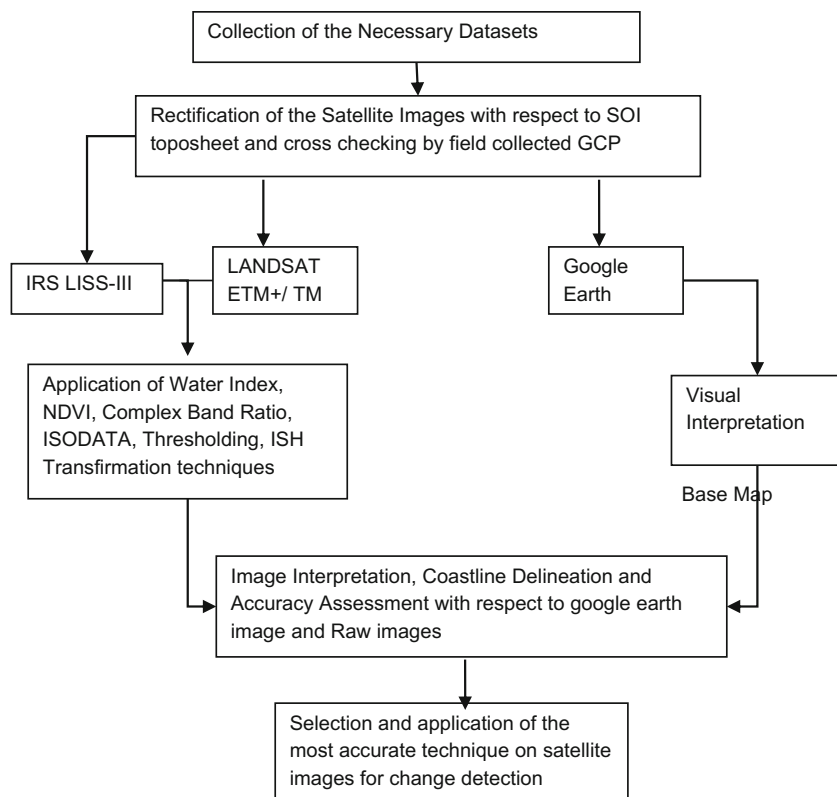
**Image processing**

In this phase of study some selected remote sensing techniques were applied for comparing the accuracy of the results. Among all corrected optical images two imageries taken from two different sensors i.e. LANDSAT ETM+ image of 2nd December 2009, and IRS 1C LISS-III image of 6th December, 2009 were taken. Six image processing techniques were applied individually on these images. The brief description of the techniques is given below:

i. *Level slicing of short wave infra red band*

Level slicing or gray level slicing scrutinises the entire gray level range of a particular band and then optimise visible image enhancement by simply slicing the values in desired range (Krishna et al. 2005; Tran Thi et al. 2014). This technique is one of the most popular semi-automated image processing methods aiming to extract water and land boundaries (Braud and Feng 1998). The shoreline can be determined automatically by level slicing of edge enhanced short wave infra red

**Fig. 2** Methodology



band through identification of land, water and transition zone classes (Krishna et al. 2005).

The SWIR band of the selected images was stacked separately. A moderate 3 × 3 edge enhancement filter was applied to sharpen the images. Edge enhancement helps in distinctive identification of coastal edge by increasing the local variance of the feature classes and minimizing the ambiguity in classifying the transition zone. Then band thresholding was done using ERDAS IMAGINE model maker. The method is shown with the help of a flow chart (Fig. 3).

After the recoding of the thematic layer final output was obtained that shows distinct boundary of land and water. Afterwards in GIS environment along the boundary, coastline was digitised

ii. *Normalised difference vegetation index*

The **NDVI** is a non-linear conversion or transformation of the visible (red) and near-infrared bands of satellite information. NDVI is defined as the difference between the visible (red) and near-infrared (NIR) bands, over their sum. The NDVI is an alternative measure of vegetation amount and condition. It is associated with vegetation canopy characteristics such as biomass, leaf area index and percentage of vegetation cover.

$$NDVI = \frac{NIR - Red}{NIR + Red} \quad (1)$$

The NDVI represents a bounded ratio value between the values -1. and +1. Healthy vegetation usually gives high reflectance in the near infrared region and low in the red visible band due to chlorophyll absorption. So these bands can be taken for the NDVI analysis. Portions of water and transitional zones are correspondingly darker in tone in both the bands (Krishana et al. 2005). The landmass having vegetation is expected to show much higher value than that of sea. Based on this logic NDVI was applied to extract the coastline and with threshold values of 0.33 and 0.20 water and land was demarcated in LISS-III and ETM+ respectively. The resultant thematic layer was then classified as land and water to a sharp shoreline.

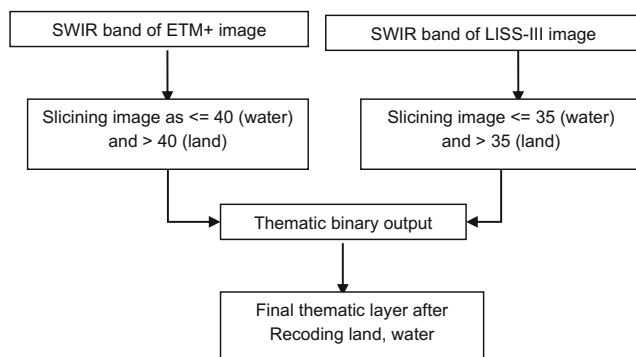


Fig. 3 Flow chart of density slicing

iii. *Complex band ratioing*

Simple band ratioing is a digital image-processing technique that enhances contrast between features by dividing a measure of reflectance for the pixels in one image band by the measure of reflectance for the pixels in the other image band (ESRI 2016). This technique has been used by different researchers as a tool to distinguish between land and water features. It eliminates effect of seasonal discrepancy of images thereby enabling extraction of water and land through their relative appearances (Masria et al. 2015). The ratio of two bands removes much of the effect of illumination in the analysis of spectral differences. Band ratio has been used in combination with output of the density slicing technique applied before to extract coastline. In the present study, accuracy of level slicing depends on the selection of correct DN value to classify the range of values in slices distinguishing between features. Any error in decision would have caused misclassification of land pixels as water causing landward intrusion of shoreline. To eliminate any of this sort of error this combination of level slicing and band ratioing could be a good option (Alesheikh et al. 2007). The entire method has been shown here using a flow chart in Fig. 4.

Multiplication of image 1 and image 2, (Fig. 4) i.e. level slicing and band ratioing results respectively should reject mistakenly classified land pixels into water in image 1 and form a new image with meaningful shoreline impression. The final output is quite comprehensive for the demarcation of coastal edge.

iv. *Water Index*

Considering the spectral reflectance pattern of soil, water and vegetation, sharp distinction between two distinctive classes, i.e., water and land as water reflectance is more in visible bands, while it mostly absorbs the infrared radiation (Krishna et al. 2005). Water Index is nothing but the sum of visible bands divided by the sum of infrared band (Braud and Feng

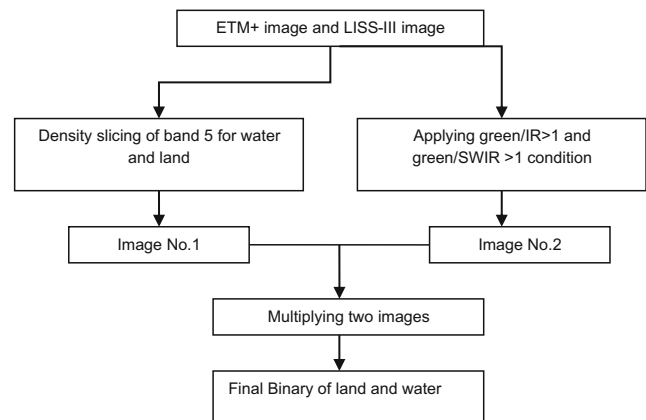


Fig. 4 Flow chart of complex band ratioing

1998). The resultant output image show three different classes, namely water, land and transition zone. The procedure aimed at obtaining the sharp edge between water and land as water reflectance is more pronounced in visible bands, while absorption is dominant in the infrared band. Using this characteristic, this technique was applied on both the images and the outputs were sliced with threshold of 2.00 in both the cases of ETM+ and LISS-III images in order to get two distinct classes of land and water. The sharp edge between the two classes refers to the coastline.

#### v. ISODATA classification

The unsupervised Iterative Self Organized Data Analysis (ISODATA) clustering algorithm is commonly implemented for classification of complex areas and is one of the most highly successful semi automated processes (Braud and Feng 1998). ISODATA clustering can be run on multi-spectral imageries with band combination of green, red, and near infra red for land/water discrimination for study area. This band combination can be used as it has consistently yielded best results in the discrimination of land cover types (Krishna et al. 2005).

Both the images were classified in 80 clusters keeping convergence value as .99 with 35 iterations limit. Then the clusters were merged as accurately as possible in two clusters of land and water. The distinct interface of the two classes represents coastline.

#### vi. Intensity hue saturation transformation

Multi-spectral images containing 3 spectral bands like green, red and near infrared usually are represented through RGB colour model. In this study, ISH colour model has been used, to represent satellite images. The formula to convert RGB to ISH is as follows:

Intensity (I)

$$I = \frac{Max+Min}{2} \quad (2)$$

Saturation (S):

$$\text{If } Max=Min \quad S=0 \quad (3)$$

$$\text{If } I \leq 0.5, \quad S = \frac{Max-Min}{Max+Min} \quad (4)$$

$$\text{If } I > 0.5, \quad S = \frac{Max-Min}{2-Max-Min} \quad (5)$$

Hue (H)

$$r = \frac{Max-R}{Max-Min} \quad (6)$$

$$g = \frac{Max-G}{Max-Min} \quad (7)$$

$$b = \frac{Max-B}{Max-Min} \quad (8)$$

$$\text{If } Max=Min, \quad H=0 \quad (9)$$

$$\text{If } R=Max, H=60(2+b-g) \quad (10)$$

$$\text{If } G = Max, H = 60(4 + r - b) \quad (11)$$

$$\text{If } B=Max H=60(6+g-r) \quad (12)$$

where the range of R, G and B is from 0 to 1.0. *Max* is the maximum value in R, G and B. *Min* is the minimum value in R, G and B. Value gaps between sea, tideland and landmass are expected in the saturation images.

The relation of saturation value between these classes can be expressed as:

$$S_{sea} > S_{tideland} \ \& \ S_{land \ area} \quad (13)$$

On the other hand in the hue(H) image, following characteristic can be found:

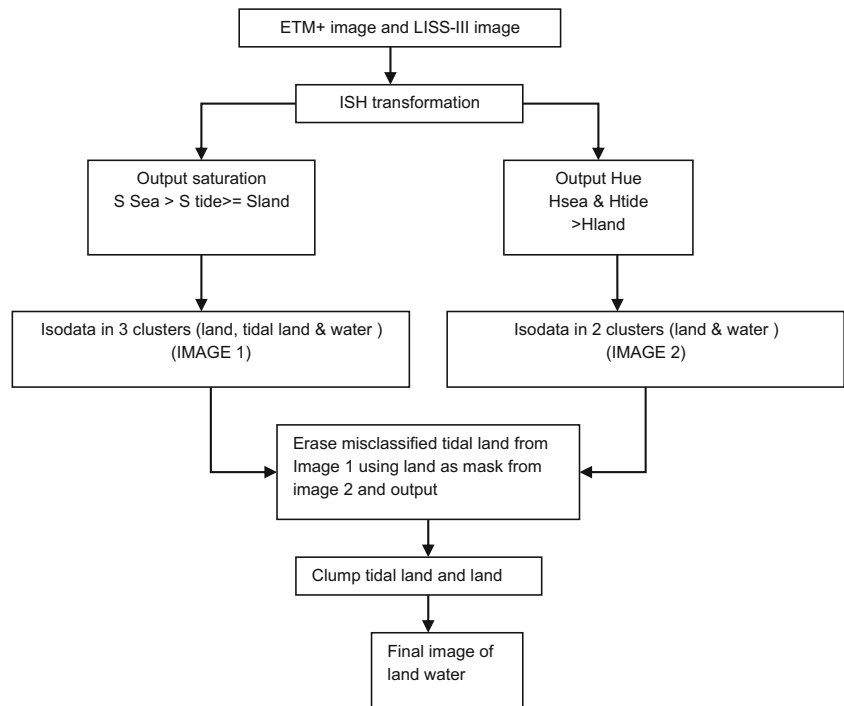
$$H_{sea} \ \& \ H_{tideland} > H_{land \ area} \quad (14)$$

Using this feature, land water boundary can be detected. The process is shown with the help of flow chart described in Fig. 5.

#### Accuracy assessment (post processing)

After applying all the techniques on images the output images were converted from continuous to thematic layer for accuracy assessment. Accuracy of the classification of land and water has been tried to be estimated in three ways, firstly with comparison to the visually interpreted high resolution google earth image, secondly field

**Fig. 5** Flow chart showing coastline extraction by ISH technique



collected GCP data of reference points of classes and thirdly the raw image itself. But problem in temporal disparity caused the constraint doing accuracy assessment from the first two reference data and maps along the coast.

For preparation of reference points field check was not useful as there was a temporal discrepancy between the satellite imagery (acquired in 2000) and present time observation. Again from visually interpreted high resolution Google Earth image with no information of the date and time of image acquisition, accuracy assessment could not be attempted due to the variations in sensors and also the difference in tidal situations of the mosaiced image. So accuracy of land water classes were tested taking referent points from the original (unprocessed) image itself. 200 reference points were taken for this purpose.

Though due to the presence of only two classes of land and water, accuracy of all the results were quite good but there were inter-techniques difference in accuracy. After comparing degree of accuracy of all the results, the best technique was selected for the detection of coastline.

## Results and discussions

### Performance of the techniques

Coastline detection has been the prior objective of the study. Some selected methods were applied on the optical images. Although all the techniques applied were able to distinguish between land and water, the area under water and land were not equal for all the outputs. Applying same techniques on both the images the output shoreline did not match with each other. Even while comparing the outputs of all the selected techniques on single image, variations were there. To assess this ambiguity, percentage of area falling under water and land for each output were assessed. For the better comparison the statistics is shown in the table below (Table 3).

This table clearly signifies that there must be variation in accuracy between different methods as no two methods give similar result in terms of percentage areal coverage of land and water. For the sake of identifying the best technique accuracy assessment (Table 4) has been done. Comparing the accuracy of the results, the best technique was obtained for the demarcation of shoreline. As there were only two classes, accuracy

**Table 3** Percentage of area of land-water in different results

| Types    | Classes | Complex band ratio | Isodata | NDVI  | Density slicing | Water index | ISH   |
|----------|---------|--------------------|---------|-------|-----------------|-------------|-------|
| LISS-III | Land    | 74.02              | 74.13   | 73.78 | 74.09           | 74.97       | 74.23 |
|          | Water   | 25.98              | 25.87   | 26.22 | 25.91           | 25.03       | 25.77 |
| ETM+     | Land    | 72.16              | 71.72   | 71.61 | 70.67           | 72.45       | 72.00 |
|          | Water   | 27.84              | 28.28   | 28.39 | 29.33           | 28.45       | 28.00 |

**Table 4** Accuracy assessment results (kappa statistics)

| Types    | Band ratio | Isodata | NDVI   | Thresholding | Water index | ISH    |
|----------|------------|---------|--------|--------------|-------------|--------|
| LISS III | 0.8682     | 0.91680 | 0.9132 | 0.9048       | 0.9561      | 0.9238 |
| ETM+     | 0.8777     | 0.9168  | 0.8379 | 0.9200       | 0.9764      | 0.8900 |

was very high for all the results. But the magnitude of differences in accuracy was considered in finding out the best technique.

As per accuracy assessment result, there are two sorts of variation in accuracy. Comparing the results from only one type of image (Fig. 6), variation is observed. Comparison between the accuracy among two different images taken from different imaging sensors also shows variation (Fig. 7). As a whole although four techniques among six, show satisfactory results namely density slicing, ISODATA classification, Water Index and ISH transformation technique, in the case of LISS-III and ETM+, respectively Water Index and Intensity-Hue-Saturation transformation technique give best results. Variation in the shorelines position in the result of the techniques applied on LISS-III image having short wave infra red in comparison with other techniques involving no SWIR band, may have caused due to the reason that the spatial resolution of SWIR (69 m) band has lower spatial resolution than other bands (23.5 m). But the output shorelines of the techniques applied that do not involve SWIR band like ISH transformation or NDVI also show disparity in shoreline position.

### Considerations

Comparing the results with other researches with similar objective always enhances understanding of the results. Sekovski et al. 2014 applied few classification techniques, i.e. ISODATA and different supervised classification algorithms on very high resolution satellite imageries to extract 40kms long shoreline facing Northern Adriatic Sea (Italy).

Result shows that the best performance was provided by ISODATA (Sekovski et al. 2014), which was found to provide considerably consistent accuracy in shoreline detection for the present study as well. ISODATA was found to be a good approach to find shoreline of different parts of the globe, including Indian coastal belt, West American Coastal tract, etc. (Braud and Feng 1998; Krishna et al. 2005; Tarmizi et al. 2014). However, Level slicing was also found to be a very useful method in identifying shoreline. It is important to mention that all of these studies were carried out on different sensors (high and moderate resolution images) over different areas. Therefore, it could be rightly commented that various factors, viz. Sensor resolution, location and type of coast under study, etc. and their interplay decide the accuracy of the methods applied to identify shoreline. Below is an account of various sources of errors and probable causes for performance-variations of the selected techniques applied in the present research.

Although the images used in the study, i.e. LISS-III and ETM+ images were acquired in the same year in same season with similar tidal condition, this difference in shoreline position might completely be due to the sensor to sensor variation. A probable explanation of this variation in the shoreline position from LISS-III and ETM+ image could be due to the difference in sensor characteristics in terms of spatial and radiometric resolution as LISS III data is actually a 7 bit data resampled into 8 bit. Besides, difference in the geodetic characteristics and atmospheric conditions while taking up the images, might cause this accuracy differences between sensor to sensor products. Spectral resolution here don't play

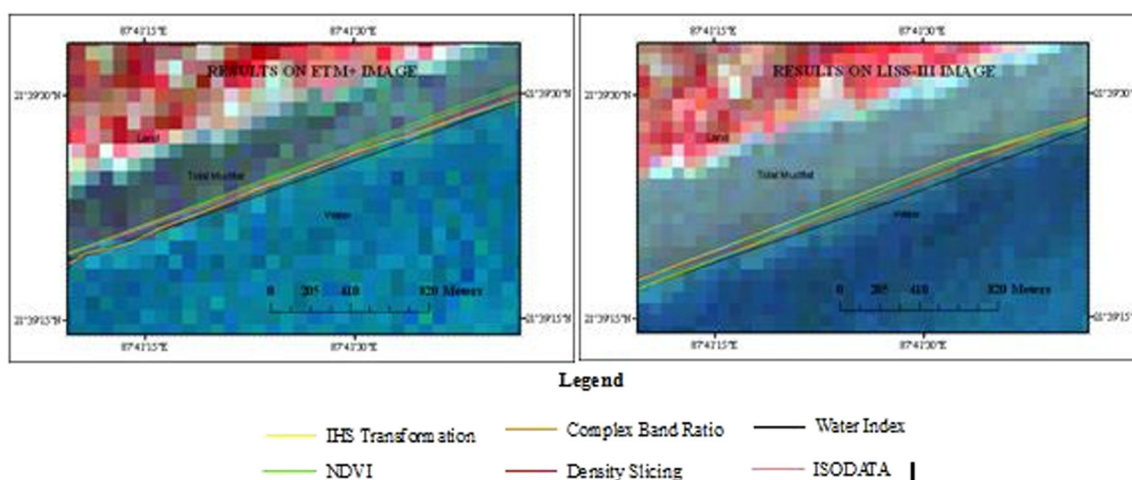


**Fig. 6** Non-uniformity in extracted shorelines using selected techniques. N.B. To portray the minute variations in shorelines, zoom level was set to very higher level. So only part of shorelines could be shown in the figure



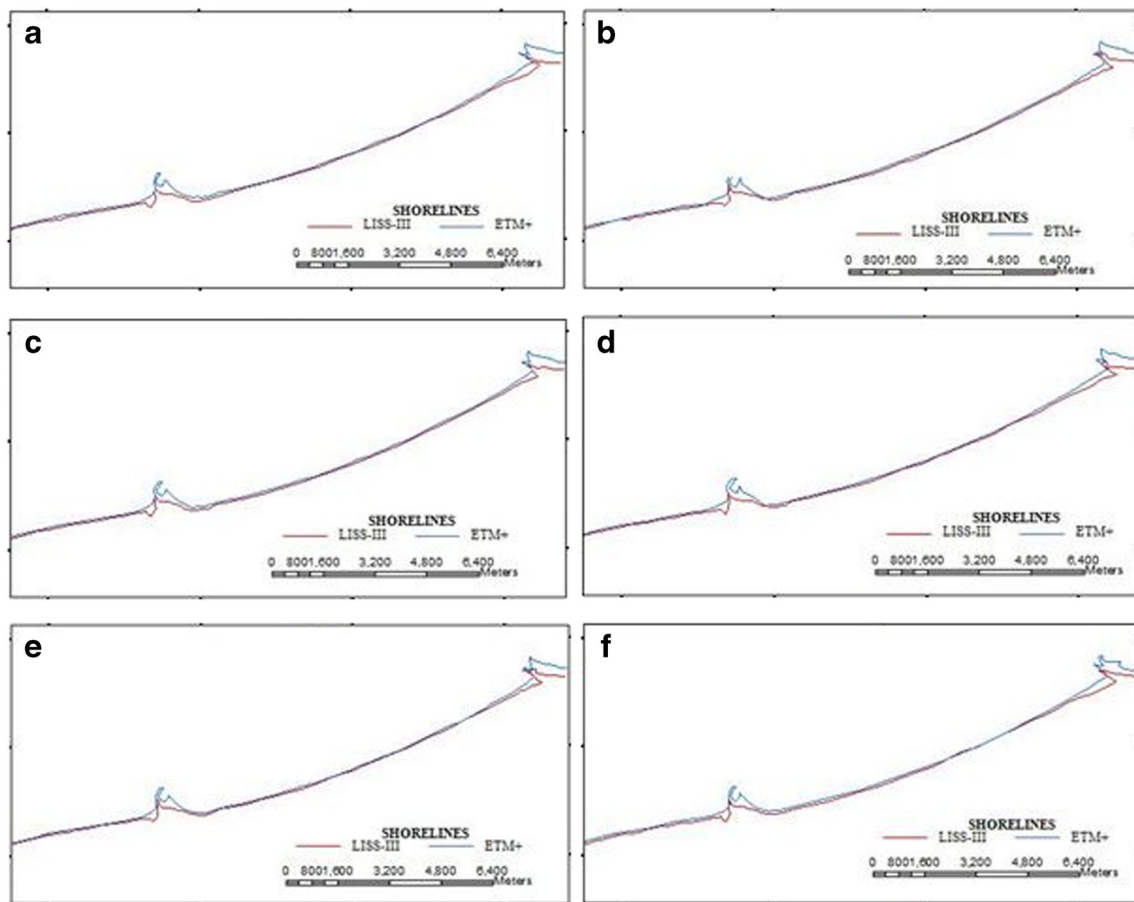


**Fig. 7** Image wise variation in shoreline positions in the outputs of applied semi-automated techniques (a) density slicing, (b) NDVI, (c) water index, (d) ISODATA, (e) ISH, (f) complex band ratio

important role as the bands from both images were taken at same resolution.

Though the works have been done with required concern and concentration some limitations are still there. The data used for change detection analysis was the images with variation in spatial resolution. So they have caused constraints towards attainment of perfection. The coastline detection techniques involving shortwave infra red band might have given certain error as the shortwave infra rd band (SWIR) resolution of LISS-III is 69 m and other bands have resolution of 23.5 m. Although down sampling from 60 m to 23.5 m was done, the resultant shoreline based on the technique using SWIR band might have faced slight shift from actual. Whether radiometric resolution difference is the cause of variation in the shoreline position on the images acquired from the different sensor or not, it could be studied if radiance count were calculated before land water classification in order to nullify the radiometric resolution impact. However, based on the research aim and objective certain results have come out which is interesting and may be replicated in other areas.

Another consideration of the results of the work is the nature of the coast under investigation and possible error of identification of shoreline sometimes is contributed by its type

itself. On wave dominated coasts, the last high tide swash line could be situated tens of hundreds of metres landward of the mean high waterline, based on the beach slope and wave energy as wave is continuously shaping the shoreline (Higgins 2005). On the other hand on tide dominated coasts, intertidal mudflats contains variations of deposits that hinders easy interpretability of the mean tidal line from photographic/imaging outputs (Anthony 2005). Both of the problems persist if we deal with mixed energy coast as our study is, with slight wave or tidal dominance. As semi automated shoreline extraction algorithms from Multispectral imageries deals with the spectral values, its accuracy depends largely upon the correct threshold selection for dividing land and water pixels (Aktaş et al. 2012). Despite being capable of yielding high performance for water delineation, error is accumulated and propagated on and through pixels which is near the water-land boundary and reflect mixed response to certain wavelengths. This causes erroneous outputs whose accuracy is much more complex to assess. All the techniques applied here depended on threshold value or range of values for shoreline delineation, Misclassification of water and land based on wrong threshold value could also contribute to the accuracy of different techniques or same techniques applied on different data.

## Conclusion

Coast line identification is a complex thing to map. It becomes even more complex when we tried to use some of the very useful and efficient algorithms on two different sensors. Among the techniques used to demarcate the line between land and water, we found the performance of these techniques varies and best method has come out to be water index with higher accuracy both when applied to LISS 3 and ETM+ images with Kappa statistics value being more than 0.95 for both the cases. However, the validity of this technique is subject to be a play of different environmental and sensor conditions and may vary.

## References

- Aedla R, Dwarkish GS et al (2015) Automatic shoreline detection and change detection analysis of Netravati-GurpurRivermouth using histogram equalization and adaptive thresholding techniques. *Aquatic Procedia* 4(0):563–570
- Ahmad SR, Lakhan VC (2012) GIS-based analysis and modeling of coastline advance and retreat along the coast of Guyana. *Mar Geod* 35(1):1–15
- Aktaş, Ü. R., G. Can, et al. (2012). A robust approach for shoreline detection in satellite imagery. 2012 20th Signal Processing and Communications Applications Conference (SIU)
- Alesheikh AA, Ghorbanali A et al (2007) Coastline change detection using remote sensing. *International Journal of Environmental Science & Technology* 4(1):61–66
- Anthony EJ (2005) Wave and tide-dominated coasts. In: Schwartz ML (ed) *Encyclopedia of coastal science*. Springer, Dordrecht
- Bhattacharya A, Sarkar SK (2001) Study on salt-marsh and associated meso-tidal beach faces variation from the coastal zone of eastern India. *Proc. of the International Conference on Ocean Engineering COE '96 IIT Madras, India, Chennai, Allied Publishing Ltd*
- Bhattacharya AK, Sarkar SK et al (2003) An assessment of of coastal modification in the low-lying tropical coast of north East India and role of natural and artificial Forcings. *International Conference on Estuaries and Coasts, Chennai*
- Braud J, Feng W (1998) Semiautomated construction of the Louisiana coastline digital land/water boundary using Landsat thematic mapper satellite imagery. *OSRAPD Technical Report Series., Louisiana, Loiusiana Coastline Digitak Spill Research and Development Program*, pp 97–102
- Chakrabarti P (1990) Process-response system analysis in the macrotidal estuarine and mesotidal coastal plain of eastern India. *Mem Geological Survey of India* 22:165–187
- Chang L-Y, Chen AJ, Chen CF, Huang CM (1999) A robust system for shoreline detection and its application to coastal-zone monitoring. In *20th Asian Conference on Remote Sensing (ACRS)*. AARS, Hong Kong
- Di, K., R. Ma, et al. (2003). Coastal mapping and change detection using high-resolution IKONOS satellite imagery. *Proceedings of the 2003 annual national conference on Digital government research*. Boston, MA, USA, Digital Government Society of North America: 1–4
- ESRI (2016) GIS dictionary. Retrieved 5th January, 2017, from <http://support.esri.com/other-resources/gis-dictionary/term/band%20ratio>
- Foody GM (2002) The role of soft classification techniques in the refinement of estimates of ground control point location. *Photogramm Eng Remote Sens* 68(9):897–903
- Frey R (1975) The realm of ichnology, its strengths and limitations. In: Frey R (ed) *The Study of Trace Fossils*. Springer, Berlin Heidelberg, pp 13–38
- Hayes MO (2005) Wave-dominated coasts. *Encyclopedia of Coastal Science*. M. L. Schwartz. Dordrecht, Springer: 1054–1056
- Higgins M (2005) Public access to the shore: public rights and private property. *America's Changing Coasts: Private Rights and Public Trust*. M. W. Diana and G. R. V. UK and USA, Edward Elgar Publishing Limited
- Jana A, Bhattacharya A (2013) Assessment of coastal erosion vulnerability around Midnapur-Balasore coast, eastern India using integrated remote sensing and GIS techniques. *Journal of the Indian Society of Remote Sensing* 41(3):675–686
- Komar PD (1976) *Beach processes and sedimentation*. Prentice-Hall, Englewood Cliffs, New Jersey
- Krishana GM, Mitra D et al (2005) Evaluation of semi-automated image processing techniques for the identification and delineation of coastal edge using IRS, LISS-III image - a case study on Sagar Island, East Coast of India. *International Journal of Geoinformatics* 1(2005)
- Krishna GM, Mitra D et al (2005) Evaluation of semi-automated image processing techniques for the identification and delineation of coastal edge using IRS, LISS-III image - a case study on Sagar Island, East Coast of India. *International Journal of Geoinformatics* 1(2005)
- Kuehl SA, Levy BM et al (1997) Subaqueous delta of the Ganges-Brahmaputra river system. *Mar Geol* 144(1–3):81–96
- Li R, Di K, Ma R (2001) A comparative study of shoreline mapping techniques. In: *The Fourth International Symposium on Computer Mapping and GIS for Coastal Zone Managemnet*. Halifax, Nova Scotia
- Masria A, Nadaoka K et al (2015) Detection of shoreline and land cover changes around Rosetta promontory, Egypt, based on remote sensing analysis. *Land* 4(1):216
- Santra A, Mitra D et al (2011) Spatial modeling using high resolution image for future shoreline prediction along Junput coast, West Bengal, India. *Geo-spatial Information Science* 14(3):157–163
- Sekovski I, Stecchi F et al (2014) Image classification methods applied to shoreline extraction on very high-resolution multispectral imagery. *Int J Remote Sens* 35(10):3556–3578
- Short AD (1983) Sediments and structures in beachnearshore environments. South E: 1st Australia. In: Mclachlan A and T Er:1Smus (eds) *Sandy beaches as ecosystems*. Junk, The Hague, p 145–155
- Tarnizi NM, Samad AM et al. (2014) Shoreline data extraction from QuickBird satellite image using semi-automatic technique. 2014 I.E. 10th International Colloquium on Signal Processing and its Applications
- Tran Thi V, Tien Thi Xuan A et al (2014) Application of remote sensing and GIS for detection of long-term mangrove shoreline changes in Mui Ca Mau, Vietnam. *Biogeosciences* 11(14):3781–3795
- Umitsu M (1993) Late quaternary sedimentary environments and landforms in the Ganges Delta. *Sediment Geol* 83(3):177–186
- Winarso G, Budhiman S (2001) The potential application of remote sensing data for coastal study. *Proc. 22nd. Asian Conference on Remote Sensing, Singapore*. Available on: <http://www.crisp.nus.edu.sg/~acrs2001>
- Wright LD, Coleman JM (1973) Variations in morphology of major deltas as function of ocean waves and river discharge regions. *AAPG Bull* 57